



Gabriele Vestri, Francesco Versaci,  
Giacomo Savini, and Jaime Aramberri

Historically, the refining process of IOL (Intraocular Lens) calculation has passed through classes of formulas, which more and more accurately have determined the spherical power of an intraocular lens, but, at the same time, have lost adherence to the physical laws, which rule the behaviour of light. As an extreme consequence of this trend, a new family of IOL calculation formulas completely based on deep learning has been recently proposed: in this outermost case, the deterministic optical approach is completely neglected and the IOL power is the output of a neural network.

In a parallel pathway during the latest decades, ray-tracing methods have taken hold in physics and engineering for optical design and analysis. This approach calculates the path of rays of light through a sequence of regions with different refractive indices [1]. Simple problems can be analysed by propagating a few rays, while a more detailed analysis requires a computer to simulate

many rays. This approach allows at the same time a return to the physics of light propagation and, if accurate input data are available, to customize the IOL calculation for each patient.

The most famous IOL calculation formulas are mainly modified versions of the Gaussian formulas for a diopter followed by a thin lens. The eye is simply modelled as a spherical diopter with power equal to the average keratometry, which is calculated using only the anterior corneal radius and a refractive index that is not the stromal one, but a weighted version of that of the stroma and of the aqueous. This is a trick to include the effect of the posterior corneal radius when this measurement is not available, but this is a valid approximation only if the ratio between the anterior and the posterior corneal radii (Gullstrand's ratio) is that of the average eye (i.e. 1.22). Therefore, most of the IOL formulas neglect the measurement of the posterior corneal surface. This was surely necessary when tomographers were not available on the market. Moreover, they consider the intraocular lens as a thin lens with zero thickness characterized by a certain value of power.

---

G. Vestri (✉) · F. Versaci  
CSO s.r.l., Florence, Italy  
e-mail: [g.vestri@csoitalia.it](mailto:g.vestri@csoitalia.it); [f.versaci@csoitalia.it](mailto:f.versaci@csoitalia.it)

G. Savini  
IRCCS Bietti Foundation, Rome, Italy

Studio Oculistico d'Azeglio, Bologna, Italy  
e-mail: [giacomo.savini@startmail.com](mailto:giacomo.savini@startmail.com)

J. Aramberri  
Clínica Miranza Begitek, San Sebastian, Spain

Clínica Miranza Ókular, Vitoria, Spain  
e-mail: [jaimearamberri@telefonica.it](mailto:jaimearamberri@telefonica.it)

---

### Basic Concepts

CSO's (Costruzione Strumenti Oftalmici) approach to IOL calculation is an attempt to apply the most advanced engineering calculation method to this problem. The IOL module was made avail-

able first in 2011 for Sirius, CSO's anterior segment tomographer, which combines Placido disc and Scheimpflug camera and, then, in 2017 for MS-39, CSO's anterior segment tomographer, which integrates Placido disc with optical coherence tomography (OCT) technology.

The measured data of the ocular anterior segment, i.e. the altimetric data of the anterior and posterior corneal surfaces and of the iris, are used in combination with the altimetric data of the intraocular lens to build a three-dimensional model of the eye. In this way, the corneal surfaces are considered with their possible asymmetry, tilt, decentration and irregularities. The intraocular lenses are modelled using the nominal parameters provided by the manufacturers, their thickness is no longer neglected and possible aspherical profiles can be taken into account as well as possible toric shapes.

For each simulated ray entering the pupil of the eye, the software calculates its intersection with the first corneal surface (Fig. 39.1). At this point, it applies Snell's refraction law to get the direction of the refracted ray by knowing the incident ray, the normal of the first corneal surface at their intersection point and the refractive indices of air and stroma. The refracted ray is traced towards the posterior corneal surface and their intersection is calculated. At this point, Snell's refraction law is newly applied to get the direction of the

refracted ray in the aqueous towards the intraocular lens. This procedure is applied to every other optical interface between cornea and retina, i.e. to the surfaces of the intraocular lens.

Once the path of a bundle of rays from the outside of the eye to its retina is known, it is possible to determine the wavefront error of the examined eye by subtracting the optical path length of the whole bundle of rays from that of an ideal aberration-free optical system.

In addition to defocus and astigmatism or, in other words, refraction (sphere, cylinder, axis and spherical equivalent), a great amount of optical information of the analysed eye can be extracted from the wavefront error:

- *Refractive map*: this map shows the refractive error for any ray passing through the pupil. This is useful to evaluate the presence of possible defocus, astigmatism and asymmetries in the optical ocular system.
- *Point spread function (PSF)*: the PSF is the impulse response of an optical system (in this case the eye after the IOL implant) to a luminous infinitesimal spot at an infinite distance. It provides the clinician with a visual method to understand the effect of aberrations on the ocular system. Ideally, the PSF should be a tiny circular point for an aberration-free optical system. Its shape is distorted and its dimen-

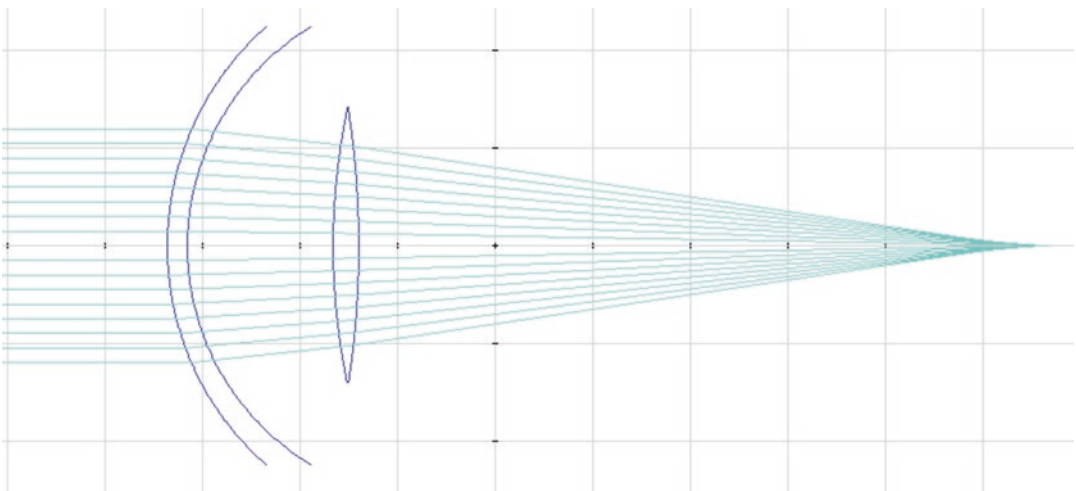


**Fig. 39.1** Ray tracing: two-dimensional simplified model of cornea and IOL

sions are enlarged by the presence of aberrations. For example, astigmatism tends to make the PSF a line whose orientation is the direction of the astigmatism; coma gives it the aspect of a comet. Just to keep in mind a numerical reference, the size of the PSF should be less than 1' for getting a visual acuity of 1.0 or less than 0.5' for getting a visual acuity of 2.0.

- Focusing chart:** this chart contains, for the selected intraocular lens, the curve for the merit figure of visual acuity obtained with various corrections of the sphere (Fig. 39.2). From a different point of view, the focusing chart shows how the visual acuity varies at the various distances of the observed object. This chart is therefore useful to evaluate the depth of field for the pseudo-phakic eye. The wider the curve, the wider the interval where visual acuity is kept near its best-corrected value. The higher the curve, the higher the best-corrected visual acuity. The dotted curve shows the diffraction-limited case, i.e. the ideal limit of an aberration-free system. This constitutes a superior limit, which cannot be reached by real eyes. Of course, the simulation does not consider the neurological component of vision, but only the optical one.

The ray-tracing calculation is done by the software for each available power of the selected IOL model. The previous results are shown for the lens, which best satisfies the requirement of the target equivalent sphere chosen by the surgeon. They can also be consulted by the user for the lenses whose powers are included in an interval centred on the power of the best lens. If the IOL model is toric, the software also makes the results available for each of the available IOL cylinders. The software proposes the axis of the astigmatic component of the WFE (wavefront error) as the default option for the IOL orientation. The user can manually change this axis if necessary.

Ignoring the complexity of the whole wavefront, paraxial IOL formulas can only provide the predicted spherical equivalent or, at most, a predicted cylinder applying the same method to two ocular meridians. It is obvious that this prediction is reliable only if the ocular surfaces (anterior corneal surface, posterior corneal surface and IOL) are regular toric surfaces, aligned on the same axis, with no tilt, with the same orientation of their principal axes or, at least, there are no significant deviations from the previous ideal conditions.

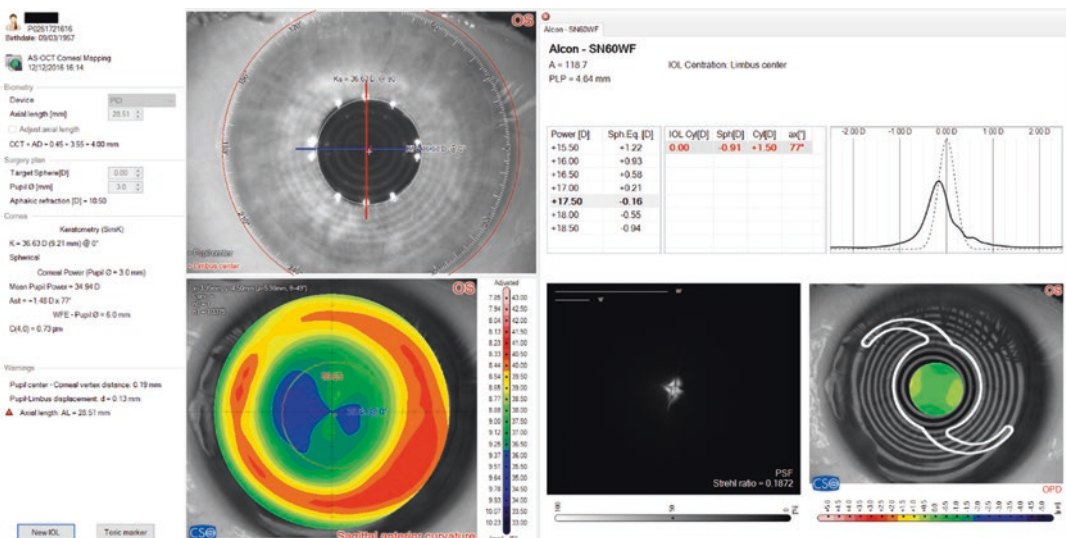


**Fig. 39.2** IOL calculation screen. Left column: relevant indices. Central column: iris frontal view with SimK values and sagittal curvature map. Right column with four different sections: IOL power and expected spherical

equivalent and refraction data (top left); focusing chart (top right); PSF (bottom left); OPD or refractive error map (bottom right)

## Prediction of the IOL Position

One of the most important sources of the refractive error in the selection of the IOL power is certainly the prediction error of the IOL postoperative position.

Third- and fourth-generation formulas generally try to predict this value by multiple regression analysis based on parameters such as the preoperative axial length, corneal curvature radius, anterior chamber depth, crystalline lens thickness and so on. Their predicted value ELP (Effective Lens Position) is not a real geometric distance between two ocular optical interfaces, but is a fictitious distance of the thin lens from the corneal vertex and serves only to make the calculation effective. Because of its nature, it cannot even be checked by a measurement in the postoperative tomographic examination.

On the contrary, when a ray-tracing approach or paraxial thick lens formulas are adopted, it is necessary to predict the real position of the implanted lens. CSO's software makes this prediction by considering some iris points on the external perimeter of the iris, which are used to calculate a best-fit plane whose tilt and position are used as an estimation of the plane where the IOL will lie after the implant. In the case of Sirius, the fitted points are the vertices of the iridocorneal angles, i.e. the intersection points between the posterior corneal surface and the anterior surface of the iris. In the case of MS-39, the fitted points are the intersection points between the anterior surface of the iris and the line passing through the scleral spur and perpendicular to the posterior corneal surface. The position of the best-fit plane is then adjusted by the A-constant, which is an indicator of the "position trend" of a certain IOL model. The predicted value PLP (which stands for Predicted Lens Position) is a real geometric distance, i.e. the distance between the posterior corneal surface and the anterior surface of the IOL.

## Performing the IOL Power Calculation

The IOL calculation module is launched from the IOL icon in the main menu display. The screen is divided into three sections (Fig. 39.2). The left one contains the main indices involved in IOL power calculation: biometry figures, where the user has to input manually the axial length and choose the type of biometer (partial coherence interferometry or immersion/applanation ultrasound); surgical plan, where target refraction and pupil size are selected; corneal powers, both keratometry and raytraced total values. The central column contains two graphic representations: the SimK indices over the iris frontal image and a selectable corneal map, either the keratometry or the total refractive power. The right column is the space where the results of the optical calculation are shown.

Once the axial length is input and target refraction and pupil size are accepted, the software allows to choose the IOL model. In this window, the IOL constant is checked and the predicted lens position (PLP) is calculated. Sometimes, the software cannot satisfactorily identify the angle structures (scleral spur and iris root in the case of MS-39 or iridocorneal angles in the case of Sirius) and requires manual editing to give way to the PLP calculation (Fig. 39.3). After that, the above-mentioned results show up in the right column of the screen distributed in four panels:

- The selected IOL and the predicted refractive result, both in spherical equivalent and spherocylinder notation;
- The PSF display with the calculated Strehl ratio;
- The OPD (optical path difference) or WFE (wavefront error) map (or the refractive error map) calculated for the measured pupil;
- The focusing chart.

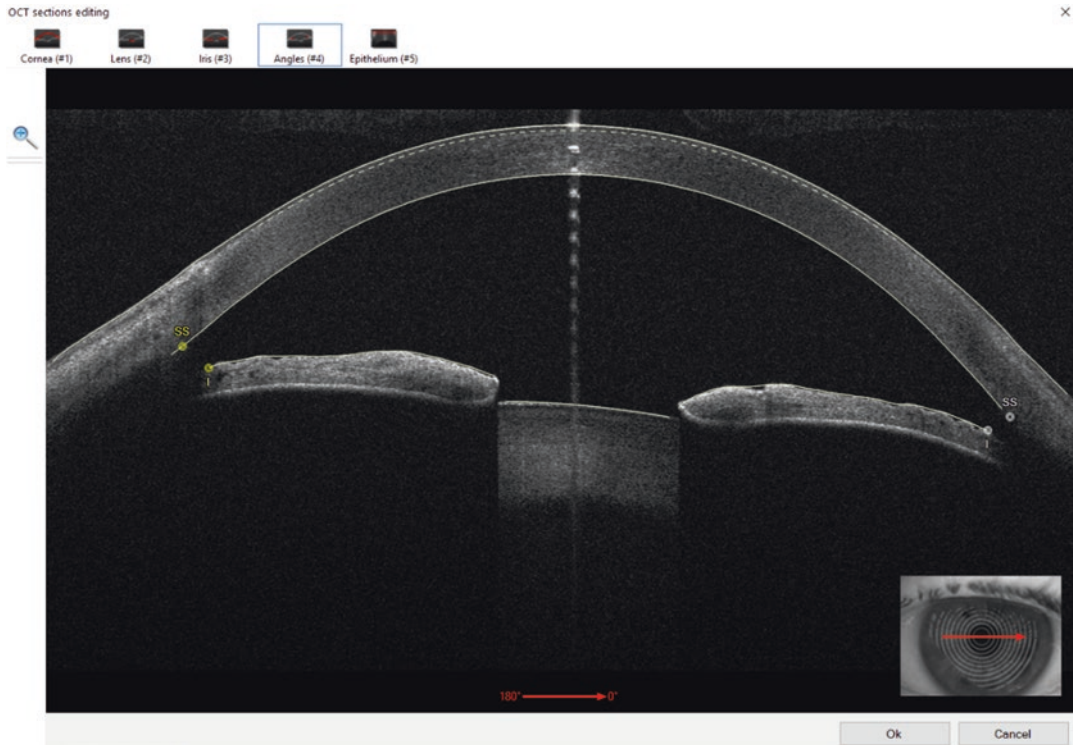


**Fig. 39.3** Scleral spur (SS) and iris root (I) manual identification

## Examples of Application

CSO's IOL module was created to manage a wide range of eyes, in particular those that underwent corneal refractive surgery [2] and highly astigmatic and/or irregular corneas.

In post-refractive surgery cases, the traditional IOL formulas are affected by three main sources of errors. First, inaccurate estimation of corneal power from the keratometry of anterior corneal surface occurs when the classical keratometric index of 1.3375 is adopted (“keratometric index error”). Second, if the chosen keratometry is SimK, corneal power is extracted from the values of the axial curvature map in a paracentral ring-shaped zone, which may partially overlap with the surgical transition zone in cases where the optical zone is small or decentered (“radius error”). Third, incorrect estimation of the ELP by thin-lens IOL power calculation formulas occurs when the post-refractive surgery anterior corneal radius is used as a predictive factor, such as in the

case of the Hoffer Q, Holladay 1, Holladay 2 and SRK/T formulas (“formula error”). This leads to an underestimation of the ELP and thus of IOL power, which results in postoperative hyperopia. To overcome these problems, several methods have been proposed. For example, the Double-K method [3] uses the anterior corneal radius before refractive surgery to estimate the ELP and its value after refractive surgery for the IOL power calculation by the vergence formula. Although it is a reliable method, it requires the knowledge of historical data and, if those are unavailable, the method cannot be applied. Conversely, CSO's method is not influenced by the keratometric index error, because it applies ray tracing to the measured three-dimensional height data of corneal surfaces with the proper refractive index for each ocular medium. In addition, the prediction for IOL position is not impaired by previous refractive surgery, because it does not consider the anterior corneal curvature, but it is based on iris reference points, which are not modified by

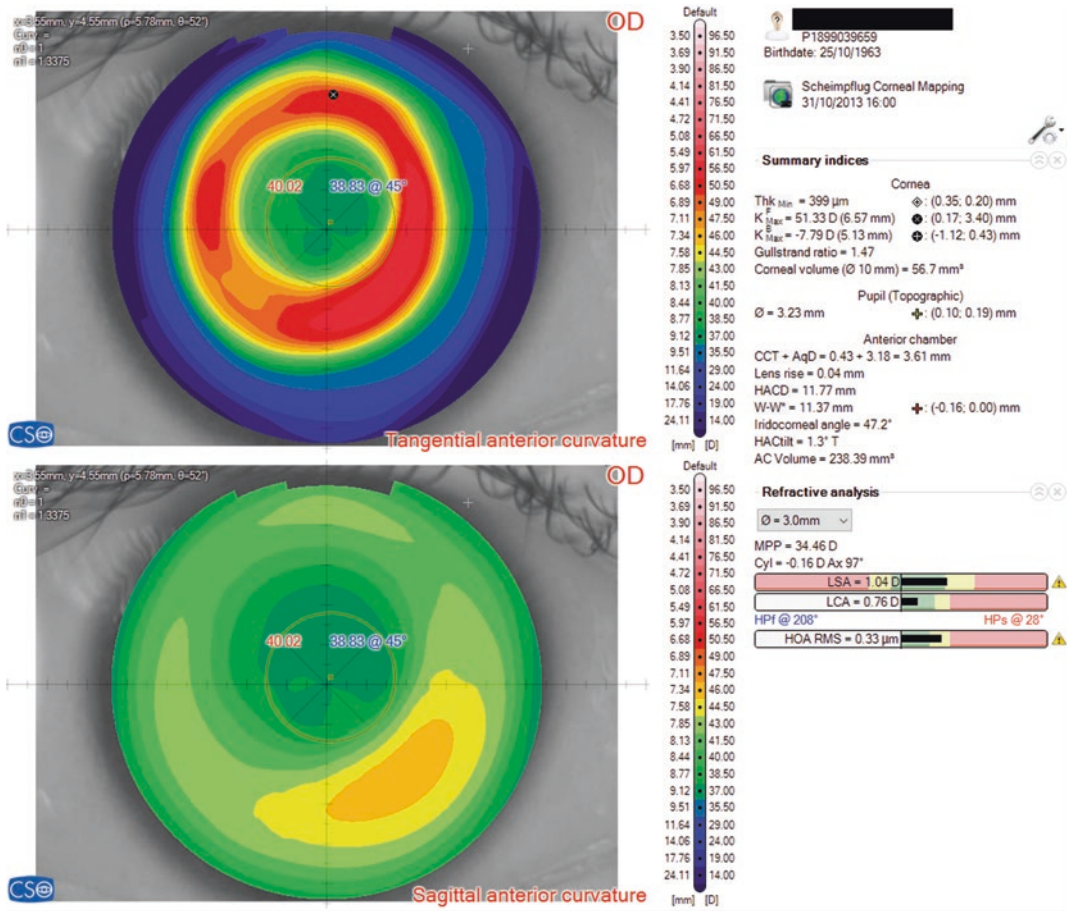


**Fig. 39.4** Post-LASIK surgery case

this kind of surgery. The prediction error of the IOL position is therefore theoretically the same in all kinds of eyes.

In Fig. 39.4, the case of a myopic eye, which underwent LASIK surgery, is shown. The tangential curvature maps clearly show that the optical zone is neither very well centred with respect to the corneal vertex nor to the pupil vertex. The average value for the SimK is 39.42 D; the mean pupil power, which is the total corneal power calculated through ray tracing within the pupil diameter of 3 mm, is 34.46 D. This big difference is due to the calculation zone for the SimK, which is an annulus centred on the corneal vertex with internal and external radii of about 1 and 1.8 mm, respectively, on an average cornea (Fig. 39.5). In this case, as in many other cases, the calculation

zone includes a portion of the surgical transition zone where the curvatures are steep, and this portion is not in the pupillary zone when the pupil is in photopic conditions. This is a further reason, in addition to the invalid hypothesis beyond the keratometry index (Gullstrand ratio is here 1.47), which makes the SimK value a wrong choice for the IOL calculation in this case and similar ones.

CSO's software considers the portion of the cornea within the actual pupil of the patient to perform ray tracing. The axial length of this eye was 30.28 mm and it was chosen to implant an Alcon SN60WF with a power of 17 D. The PLP was 4.31 mm while the real position turned out to be 4.41 mm. This denotes good behaviour of the predictive algorithm for the IOL position. The predicted refraction was  $-2.59 + 0.21 \times 180$ ,

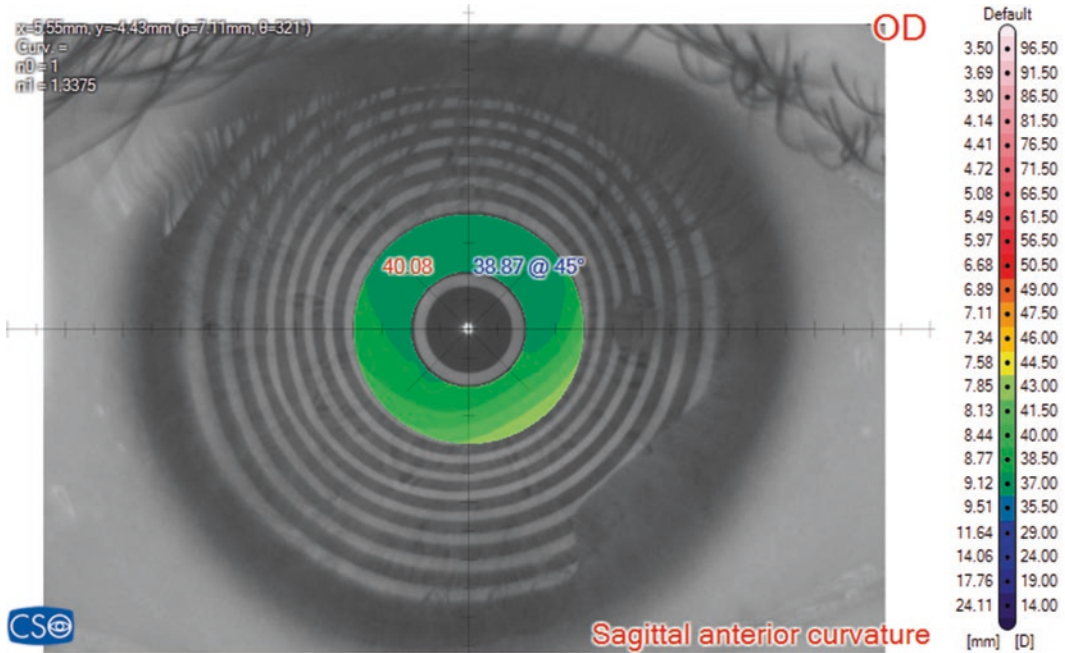


**Fig. 39.5** Annular region of sagittal (axial) curvature map used to calculate the values of SimK. The annulus, centred on the corneal vertex with internal and external radii of about 1 and 1.8 mm on an average cornea, includes a portion of the surgical transition zone where the curva-

tures are steep. The values of SimK are not a proper choice for IOL calculation also because they include the effect of the surgical transition zone, which is external to the pupil region in photopic conditions

which is rather similar to the measured subjective refraction  $-2.75 + 0.5 \times 5$ .

Another typical case where the IOL module can be useful is shown in Fig. 39.6. This is the case of an eye, which underwent PRK (photorefractive keratectomy) to correct a hyperopic defect of about 3 D. The Gullstrand ratio is here 1.11, quite lower than the mean normal value. Even in this case, the calculation assumptions of keratometry, in particular the value of the keratometric index, lose their validity. Furthermore, the value of curvature modified by PRK leads many formulas to a wrong prediction of the IOL position. CSO's predicted position (3.57 mm), which is based on anatomical structures not altered by surgery, was close to the actual one (3.69 mm). The predicted refraction was  $-1.82 + 0.93 \times 106$  (Fig. 39.7), while the subjective refraction was  $-1.50 + 0.75 \times 90$ . The equivalent spherical error was  $-0.23$  D and could be almost zeroed if we would input the actual position in the software. In this case, it appears that the residual error on

refraction can be fully ascribed to the error on the estimated IOL position.

As regards astigmatic corneas, CSO's method is able to manage correctly both anterior and posterior corneal surfaces, which may be not coaxial, have a different orientation of the astigmatism and a pupil position relatively displaced from the corneal vertex.

The case shown in Fig. 39.8 is an eye with a toric cornea. The total corneal astigmatism calculated through the WFE over a pupil diameter of 3 mm is with-the-rule  $+3.36 \times 114$  and derives from the contributions of the anterior and posterior components, respectively,  $+3.78 \times 113$  and  $+0.44 \times 16$ .

The implant of a non-toric intraocular lens would leave a cylinder too high to be borne by the patient without the help of spectacles or contact lenses. This is clear from the refraction table and, for an expert eye, from the OPD/WFE map. The use of a toric IOL would allow cancelling almost totally the cylinder. The predicted

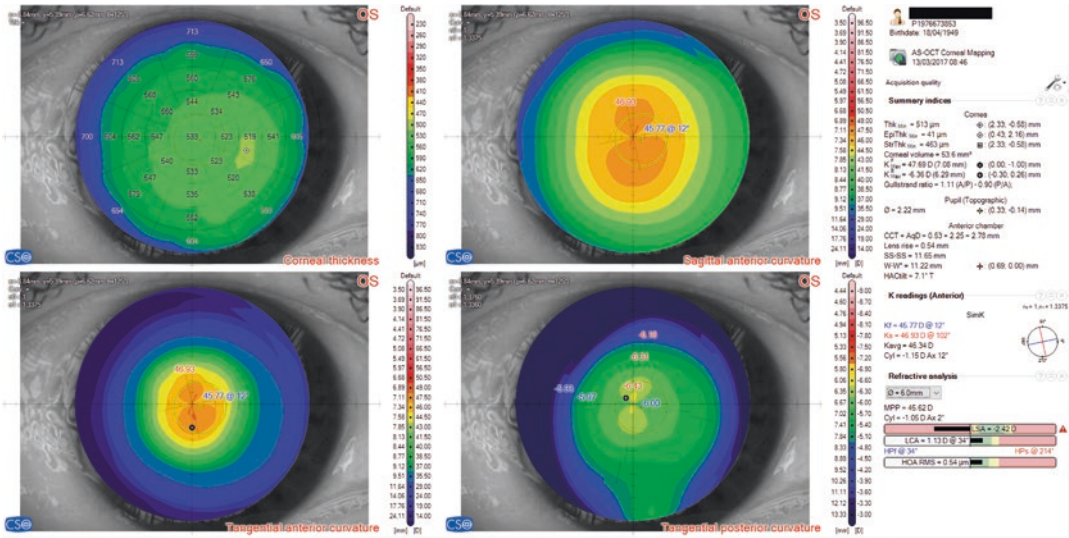


Fig. 39.6 Overview of the topographic maps for an eye, which underwent PRK in order to correct a hyperopic defect

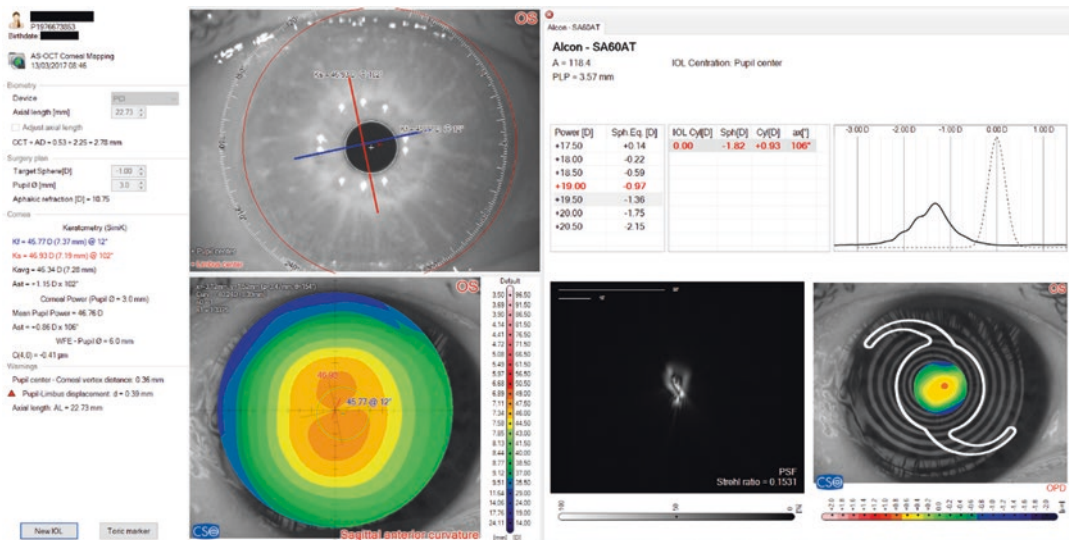


Fig. 39.7 IOL calculation for the eye, which underwent PRK in order to correct a hyperopic defect

refraction is  $-1.05 + 0.37 \times 110$  with an IOL cylinder of 4.5 D (Fig. 39.9). Unfortunately, the clinician chose to implant a cylinder ( $-3.75$  D) inferior to the one suggested by this software and the patient showed a residual cylinder of 1 D after the IOL implant ( $-1 + 1 \times 125$ ). This case shows a very good agreement between the actual subjective refraction and the one predicted by the software, as it appears in the residual cylinder of  $+0.88 \times 112$  calculated for the

IOL with a cylinder equal to the implanted value.

CSO's IOL module is also theoretically designed to manage correctly even more irregular corneas like the keratoconic or post-graft ones. Eyes after DMEK (Descemet Membrane Endothelial Keratoplasty) or DSAEK (Descemet's Stripping Automated Endothelial Keratoplasty) are likely to suffer problems similar to those of post-refractive surgery eyes when



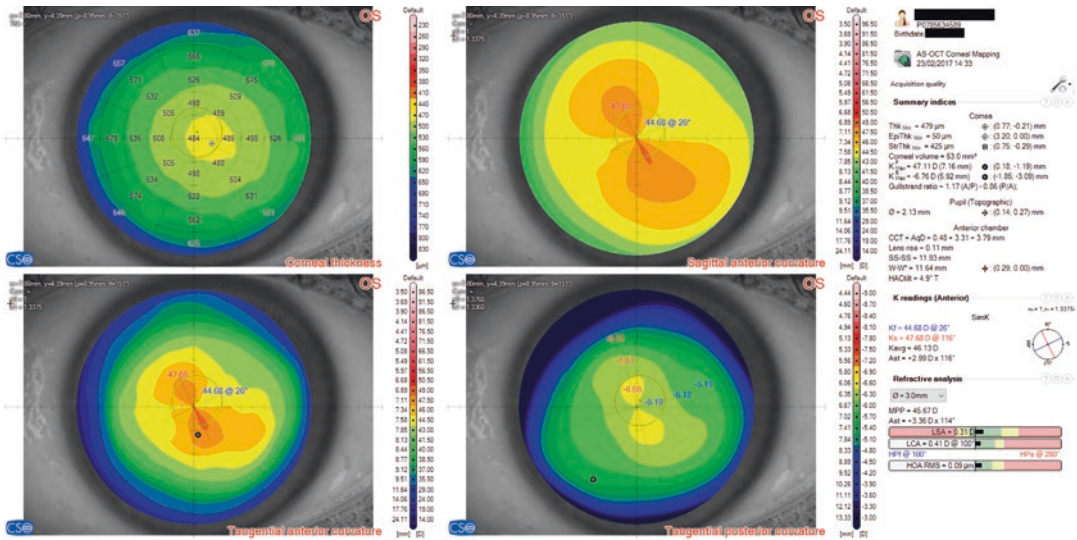


Fig. 39.8 Overview of the topographic maps for a toric cornea

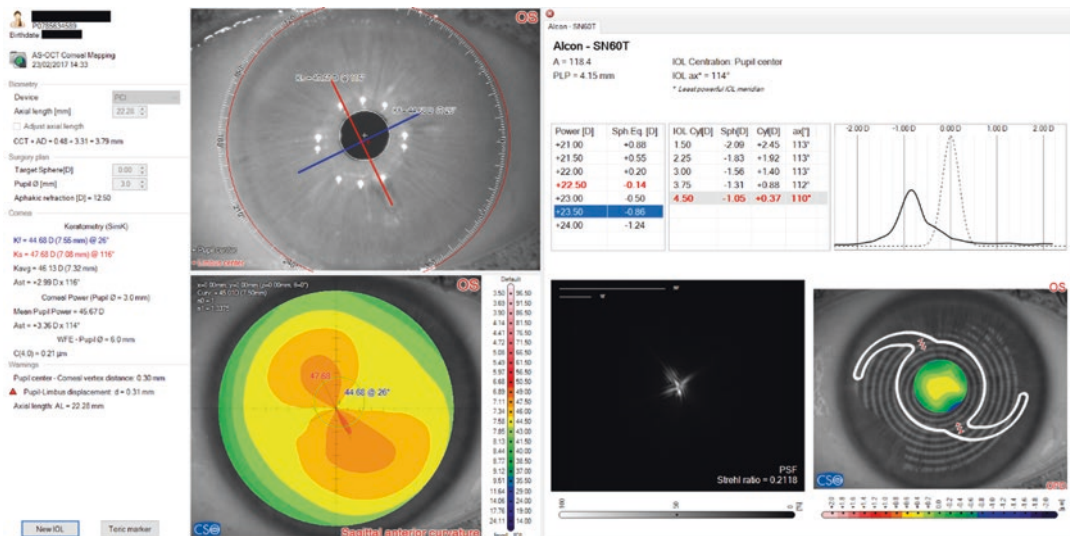


Fig. 39.9 IOL calculation for a toric cornea where a toric model was chosen for the implant. The table at the centre of the screen contains the predicted spherical equivalent

for the various IOL powers; the table at its right contains the predicted refraction for each cylinder of the selected IOL power

keratometry values are adopted as corneal power. Of course, in these cases, the measurements may be affected by more severe measurement errors, which decrease the reliability of the calculations. Nonetheless, it is to be noticed that in all these cases, the aberrations are so high that we cannot hope to reach a good visual acuity by simply correcting the sphere and cylinder through an

IOL. The software is able to highlight these cases by showing an irregular wavefront error and a flat focusing chart, which can be a useful indication for the surgeon of poor expectations for the visual acuity of the patient.

The next case we present in this chapter is an eye, which underwent an endothelial transplantation (DSA EK) before the cataract surgery

**Fig. 39.10** OCT section of the eye, which underwent DSAEK before cataract surgery. The donor tissue is clearly visible below the patient's posterior corneal surface

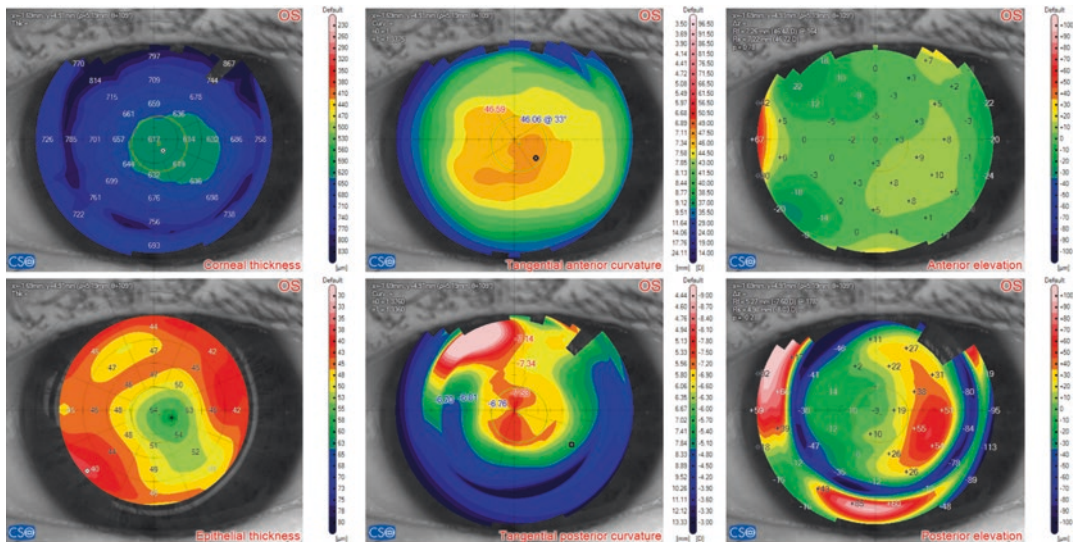
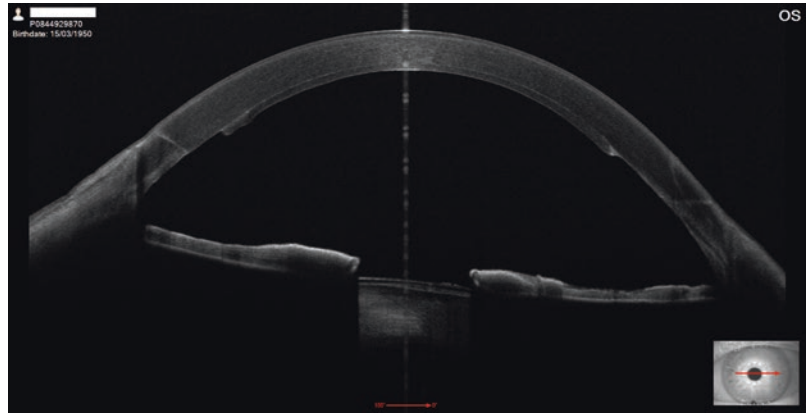


**Fig. 39.11** Overview of the eye, which underwent DSAEK before cataract surgery

(Fig. 39.10). The anterior corneal surface does not exhibit particular anomalies. It is a bit steeper than the average cornea and has a certain degree of asymmetry along the vertical direction (Fig. 39.11). The posterior corneal surface has a rather high degree of toricity, which translates into a not negligible astigmatic component of the wavefront error  $+0.81 \times 4$  (Fig. 39.12). The anterior astigmatic component is  $+1.06 \times 74$ . The two astigmatic components out of phase of  $70^\circ$  produce a total corneal astigmatism of  $+0.67 \times 50$ . The Gullstrand ratio between the anterior and the posterior curvature is 1.29. The implanted IOL was an AMO Tecnis1 ZCB00 with a power of 23 D. The predicted IOL position was 4.68 mm

while the actual position was verified to be 4.49 mm after the implant. The refraction predicted by the software was  $-0.52 + 0.67 \times 50$  (Fig. 39.13) in good agreement with the subjective refraction after the surgery, which was  $0 + 0.50 \times 60$ . Even though the transplant altered the posterior corneal surface and introduced new aberrations (astigmatism in particular), greater than those of a normal unoperated eye, the software was not misled in the correct choice of the IOL.

The next example is the eye of an airplane pilot, who underwent RK (radial keratotomy) in 1989. He had a good visual quality until 2017, when he began to see the peripheral cuts of the

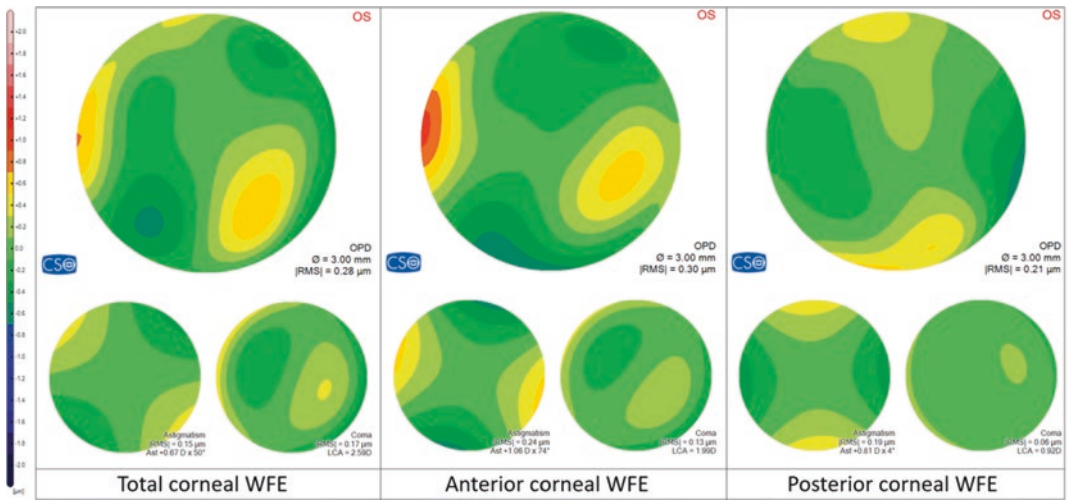


**Fig. 39.12** DSAEK case: total corneal wavefront error and its contributions from anterior and posterior corneal surfaces. The smaller maps at the bottom of the image

show the components of astigmatism and coma for each of the WFEs shown at the top of the image

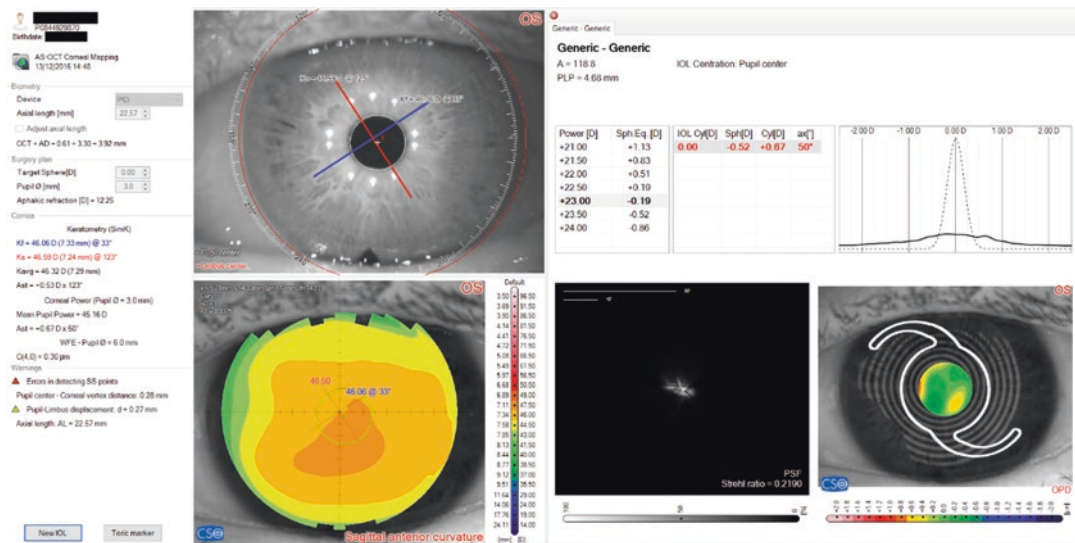


**Fig. 39.13** IOL calculation for the eye, which underwent DSAEK surgery before cataract surgery

previous surgery and some central halos, due to an incipient cataract (Fig. 39.14). An improvement of visual quality was possible by administering pilocarpine, but the vision was too dark. This condition prevented him from doing his job.

The scotopic pupil diameter was about twice the optical zone diameter (Fig. 39.15).

The preoperative evaluation led to lensectomy with the implantation of an IC-8 (AcuFocus Inc.,

California, USA). This is a single-piece hydrophobic acrylic posterior chamber IOL, which combines small aperture optics with a monofocal IOL to achieve extended depth of focus and reduce the influence of corneal aberrations. The calculation was performed with the IOL module adopting the nominal value 120.5 for the A-constant. An IOL with a power of 18 D was chosen (Fig. 39.16).

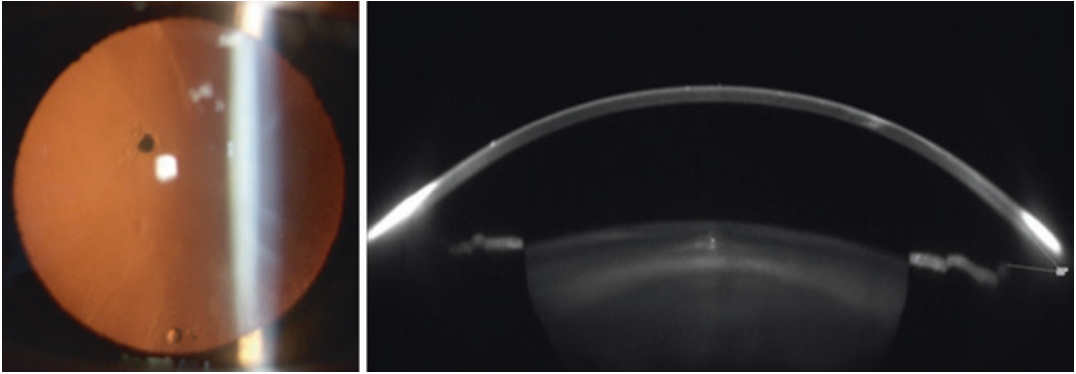


**Fig. 39.14** Slit lamp frontal image and Scheimpflug section of the post-RK case: incipient cataract is only visible in the second image

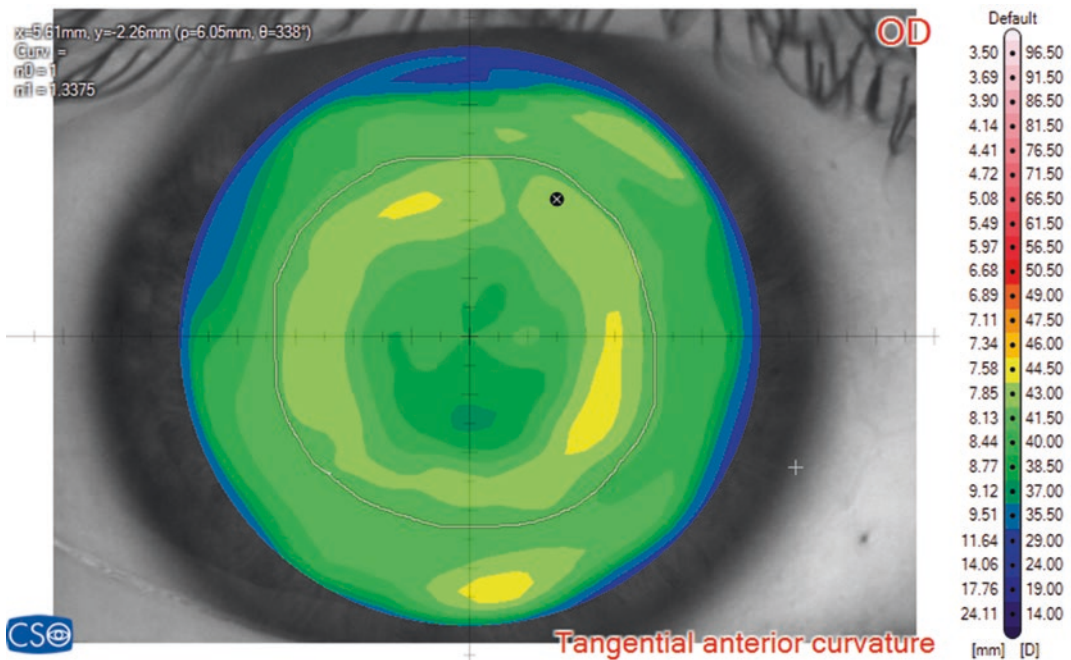


**Fig. 39.15** Tangential anterior map for the post-RK case: the scotopic pupil diameter is about twice the optical zone diameter

The predicted refraction was  $-0.27 + 0.43 \times 52$  and the postoperative outcome was emmetropy; moreover, the pinhole enabled the patient good uncorrected near vision. Halos disappeared and peripheral cuts were excluded from the optical zone by the IOL small aperture. The patient could resume his job.

The next case is an eye, which underwent PRK in 1999 for a correction of 9 D myopia. In 2019, it was necessary to recur to cataract surgery (Fig. 39.17). A monofocal IOL was implanted but the result was fairly far from the expected one: the patient complained of monocular diplopia, uncorrected visual acuity (UCVA) was 0.3

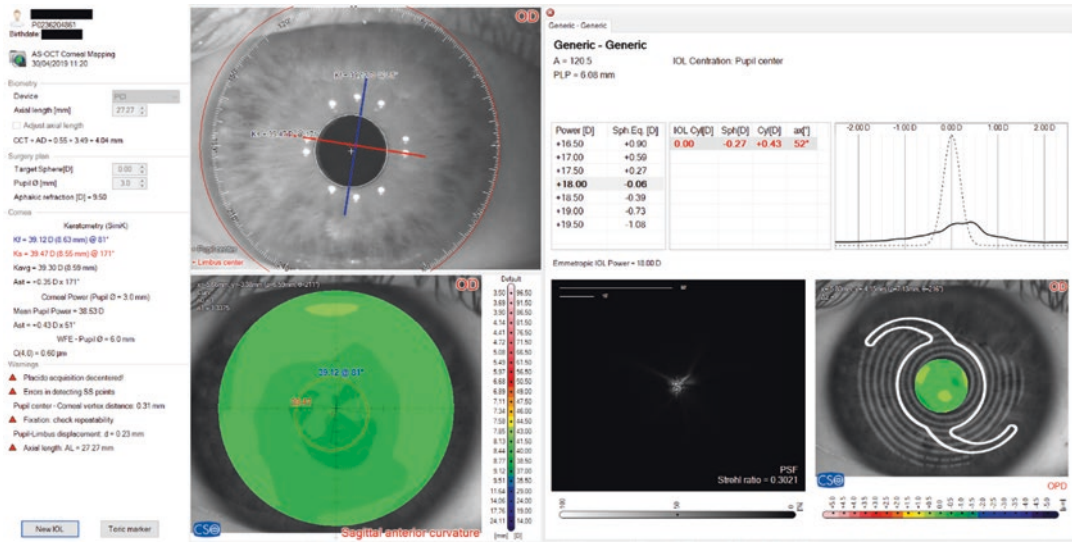


Fig. 39.16 IOL calculation for the post-RK case

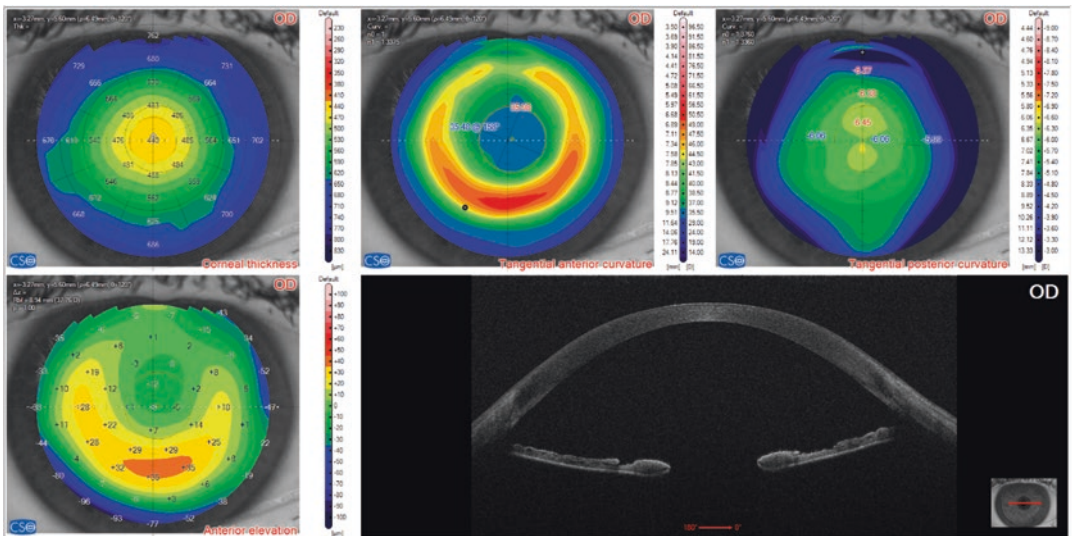


Fig. 39.17 Topographic maps and OCT section for the post-PRK eye, where the removal of the first implanted IOL was necessary

and corrected distance visual acuity (CDVA) was 0.8 with a residual hyperopic refraction (+1.75 + 0.50 × 30). The surgeon thought that the poor visual outcome was due to the combination of wrong IOL power and laser-induced corneal aberrations and proposed an IOL exchange with

the implantation of an IC-8. This time the IOL power (24 D) for a target spherical equivalent of -0.5 D was calculated by the IOL module. The predicted refraction was -0.62 + 0.15 × 36 (Fig. 39.18). The postoperative result was emmetropia with UCVA equal to 1.

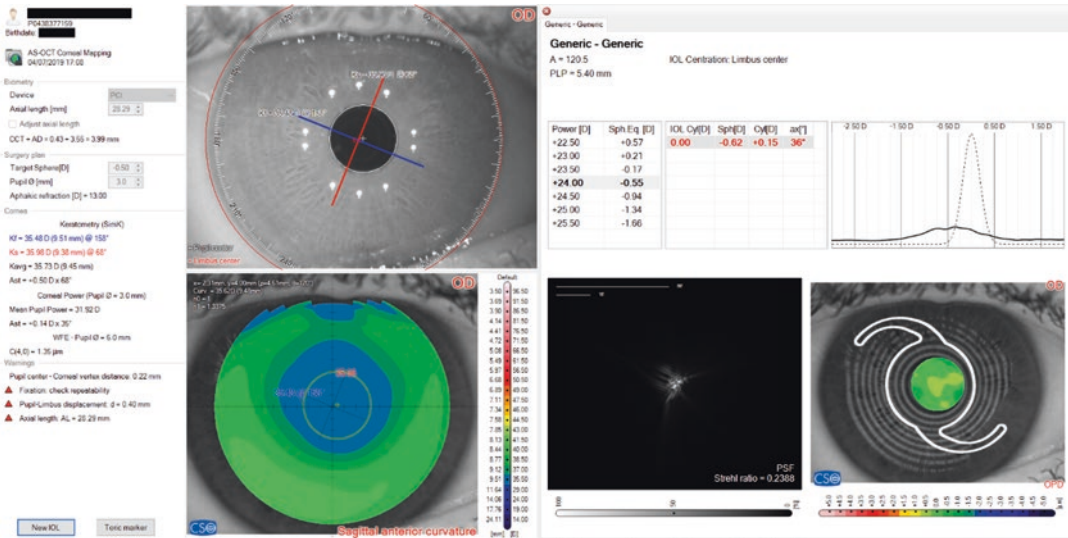


Fig. 39.18 Post-PRK case: IOL calculation for the new IOL implant

## References

- Born M, Wolf E, Bhatia A, et al. Principles of optics: electromagnetic theory of propagation, interference and diffraction of light. 7th ed. Cambridge: Cambridge University Press; 1999.
- Savini G, Hoffer KJ, Ribeiro FJ, Mendanha Dias J, Coutinho CP, Barboni P, Schiano-Lomoriello D. Intraocular lens power calculation with ray tracing based on AS-OCT and adjusted axial length after myopic excimer laser surgery. *J Cataract Refract Surg.* 2022;48(8):947–53.
- Aramberri J. Double-K method to calculate IOL power after refractive surgery. *Journal of Cataract & Refractive Surgery.* 2005;31(2):255–6.

**Open Access** This chapter is licensed under the terms of the Creative Commons Attribution 4.0 International License (<http://creativecommons.org/licenses/by/4.0/>), which permits use, sharing, adaptation, distribution and reproduction in any medium or format, as long as you give appropriate credit to the original author(s) and the source, provide a link to the Creative Commons license and indicate if changes were made.

The images or other third party material in this chapter are included in the chapter's Creative Commons license, unless indicated otherwise in a credit line to the material. If material is not included in the chapter's Creative Commons license and your intended use is not permitted by statutory regulation or exceeds the permitted use, you will need to obtain permission directly from the copyright holder.

